

Targeting Complement C5a Receptor 1 for the Treatment of Immunosuppression in Sepsis

Oliver Sommerfeld,^{1,2} Anna Medyukhina,³ Sophie Neugebauer,⁴ Mohamed Ghait,^{1,2} Svenja Ulferts,^{1,2} Amelie Lupp,⁵ Rainer König,^{2,6} Reinhard Wetzker,¹ Stefan Schulz,^{2,5} Marc Thilo Figge,^{2,3,7} Michael Bauer,^{1,2} and Adrian T. Press^{1,2}

¹Department of Anesthesiology and Intensive Care Medicine, Jena University Hospital, Am Klinikum 1, 07747 Jena, Germany; ²Center for Sepsis Control and Care (CSCC), Jena University Hospital, Jena, Germany; ³Applied Systems Biology, Leibniz Institute for Natural Product Research and Infection Biology, Hans Knöll Institute (HKI), Jena, Germany; ⁴Institute of Clinical Chemistry and Laboratory Diagnostics, Jena University Hospital, Jena, Germany; ⁵Institute of Pharmacology and Toxicology, Jena University Hospital, Jena, Germany; ⁶Network Modeling, Leibniz Institute for Natural Product Research and Infection Biology, Hans Knöll Institute Jena, Jena, Germany; ⁷Institute of Microbiology, Faculty of Biological Sciences, Friedrich Schiller University Jena, Jena, Germany

Complement factor C5a was originally identified as a powerful promoter of inflammation through activation of the C5a receptor 1 (C5ar1). Recent evidence suggests involvement of C5a not only in pro- but also in anti-inflammatory signaling. The present study aims to unveil the role of C5ar1 as potential therapeutic target in a murine sepsis model. Our study discloses a significantly increased survival in models of mild to moderate but not severe sepsis of C5ar1-deficient mice. The decreased mortality of C5ar1-deficient mice is accompanied by improved pathogen clearance and largely preserved liver function. C5ar1-deficient mice exhibited a significantly increased production of the pro-inflammatory mediator interferon- γ (IFN- γ) and a decreased production of the anti-inflammatory cytokine interleukin-10 (IL-10). Together, these data uncover C5a signaling as a mediator of immunosuppressive processes during sepsis and describe the C5ar1 and related changes of the IFN- γ to IL-10 ratio as markers for the immunological (dys)function accompanying sepsis.

INTRODUCTION

The immune system gathers a wide range of adaptive and innate responses in order to protect against external and internal threats encountered by the human body. The innate immune response consisting of both cellular components and humoral factors acts as the first line of defense against invading pathogens. The complement system as part of the humoral innate immune response contributes primarily to clearance of cell debris.¹ However, in systemic inflammatory states, including sepsis, a profound activation of the complement system has been observed contributing to organ damage.² On the other hand, the complement adds to organ regeneration, neuroprotection, and the generation of hematopoietic stem cells.³ Besides its role in pro-inflammatory responses, complement activation has also been described to promote immunosuppressive effects, indicating a crucial role of the complement system during immune homeostasis in health and disease.⁴

During complement activation, complement factor C5 is enzymatically cleaved and gives rise to multiple products, including the anaphylatoxins C5a and C5b. C5a typically functions as a pro-inflammatory peptide and exerts its effects by interacting with C5a receptor 1 (C5ar1, also known as CD88) and C5a receptor 2 (C5ar2, also known as C5L2 and GPR77).⁵

After activation of C5ar1, several downstream cascades are initiated, depending on the cell type. In neutrophils, phosphoinositide 3-kinase (PI3K) is activated, provoking nicotinamide adenine dinucleotide (phosphate) (NAD(P)H) oxidase assembly, which contributes to the clearance of invading pathogens.^{6,7} Previous work revealed that the exposure of neutrophils to high doses of C5a perturbed C5ar1 downstream signaling and neutrophil function.^{8–10} Interestingly, treatment of macrophages with high amounts of C5a led to the release of anti-inflammatory mediators, indicating ambivalent functions of the anaphylatoxin in the inflammatory response.^{11,12} Notably, some bacteria use strategies for blocking the complement system in order to persist in their host.¹³ For instance, de Haas and co-workers¹³ subjected mice to intravenous injections of chemotaxis inhibitory protein of *Staphylococcus aureus* followed by intraperitoneal injection of C5a, which resulted in inhibition of the C5a/C5ar1 interaction with chemotaxis inhibitory proteins (CHIPS) and prevented the recruitment of phagocytic cells in this mouse peritonitis model.

These observations are consistent with the presence of a second C5a receptor, C5ar2, with anti-inflammatory function. The exact function of C5ar2 receptor is less well understood, and previous studies (Gao et al.,¹⁴ Rittirsch et al.,¹⁵ and Wang et al.¹⁶) suggest its function as a decoy receptor as well as a receptor for C5a-associated

Received 3 January 2020; accepted 1 September 2020;
<https://doi.org/10.1016/j.ymthe.2020.09.008>

Correspondence: Adrian T. Press, Department of Anesthesiology and Intensive Care Medicine, Jena University Hospital, Am Klinikum 1, 07747 Jena, Germany.
E-mail: adrian.press@med.uni-jena.de

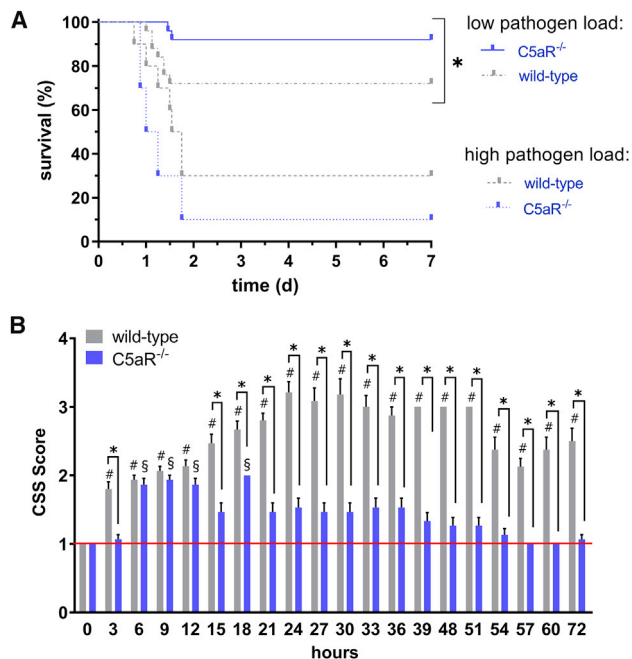


Figure 1. C5ar1 Deficiency Improves Survival in a Mild Sepsis Model

(A) Survival rate of C5ar1 knockout (C5aR^{-/-}) mice compared to wild-type mice subjected to low pathogen load (7.76×10^5 total CFU/g body weight; mild to moderate sepsis) or high pathogen load (1.21×10^6 total CFU/g body weight; severe sepsis) of a polymicrobial human fecal slurry. **Statistical difference between indicated groups ($p < 0.05$, log-rank test, low pathogen load: 25 mice/group; high pathogen load: 10 mice/group). (B) Beneficial outcome and less clinical severity (CSS Score) were observed in C5aR^{-/-} mice under low pathogen load. Data are displayed as mean barplot + SEM. §C5aR^{-/-} or #wild-type significant to respective time point 0, $p < 0.05$, one-way ANOVA with Tukey test correction; *significant difference between C5aR^{-/-} and wild-type at individual time points, $p < 0.05$ Student's t test, 15 mice/group.

immunosuppression. The C5a/C5ar2 signaling is also crucial during lipopolysaccharide (LPS)-induced shock and leads to an increased susceptibility to LPS.¹⁷

C5ar1 and C5ar2 expression increases in the lung, kidney, heart, and liver tissue early after polymicrobial sepsis in mice.^{14,18} The development of multiple organ failure during sepsis includes or is even propagated by liver dysfunction, and this is associated with a poor outcome.¹⁹ Complement components including C5a are central activators of Kupffer cells (KCs), which subsequently release interleukin-1 β (IL-1 β) and IL-6, further promoting the infiltration of neutrophils, a hallmark of liver injury associated with sepsis.^{20,21} The ensuing hepatocellular injury develops rapidly, resulting in excretory dysfunction of the liver and subsequent cholestasis.^{22–24} Previous studies linked early liver dysfunction in sepsis to increased PI3K signaling, and knockout of the PI3K species gamma (PI3K γ) was shown to protect against liver dysfunction in sepsis.²⁴ Previously, a clinical study revealed that high levels of C5a correlate with increased mortality in human sepsis.²⁵ The importance of the C5a receptors (C5ar1 and C5ar2 [C5L2]) has been further highlighted in a mid-grade cecal

ligation and puncture sepsis model. In these studies, the knock-out or blockage of the receptors individually (before sepsis) protected against development of multiorgan failure and reduced mortality.^{9,15}

Among the complement components, the anaphylatoxin C5a has been proven to elicit one of the strongest inflammatory responses. However, previous studies also indicate immunosuppressive effects, primarily attributed to signaling through C5ar2.¹⁶ Our current study aims to elaborate involvement of these opposing functions of C5a signaling in septic organ failure. Unexpectedly, the data disclose C5ar1 as a mediator of the immunosuppressive activities of the complement system in septic mice.

RESULTS

Effects of C5ar1 Knockout (C5aR^{-/-}) on Survival and Disease Progression

BALB/c mice were infected with two different loads of characterized polymicrobial feces (7.76×10^5 total colony-forming units [CFU] versus 1.21×10^6 total CFU per g body weight [BW]; Table S1), leading to different mortality rates of 30% versus 70% after 48 h, respectively. Subjecting C5ar knockout mice to the same two pathogen loads caused a decreased survival in the high-dose but a significantly increased survival in the low-dose sepsis model (Figure 1). Fortifying these results, C5aR^{-/-} improves the overall clinical condition (assessed by means of the established clinical severity score²⁶ of the animals infected with a low pathogen load) (Figure 1B). To scrutinize the pathogen load or the host response as causes of the opposing effects of different pathogen doses, we investigated the effects of an antibiotic treatment on the high-dose sepsis model 6 h after infection. The eradication of the bacteria by meropenem increased the 48-h survival of both wild-type and knockouts but did not alter the relation of the mortality of wild-type and C5aR^{-/-} observed in the absence of antibiotics (Figures S1 versus 1). These findings suggest an ambivalent role of C5ar1 in the host response during sepsis depending on the initial pathogen load.

C5aR^{-/-} Prevents Liver Failure in Sepsis

C5ar1 is widely expressed in the immune system and upregulated during inflammation (Figures S2A and S2B; Riedemann et al.¹⁸). Our results depicted that apart from immune cells, hepatocytes express C5ar1 during sepsis (Figure S2C).

Even though knockout mice are immunocompromised, the pathogen clearance from blood during sepsis is not affected, whereas the bacterial translocation to the liver parenchyma is reduced (Figure 2A). Since liver failure was previously associated with poor survival in the peritoneal contamination and infection (PCI) model used,²⁴ we investigated effects of the C5aR^{-/-} on tissue damage, especially in the liver. The C5aR^{-/-} mice subjected to low pathogen loads revealed slightly elevated alanine aminotransferase (ALT) and albumin values, which did not differ from wild-type mice (Figure 2B). The histological assessment of the tissue showed no obvious signs of liver tissue damage (Figure 2C). We noticed that C5aR^{-/-} sham mice had reduced amounts of

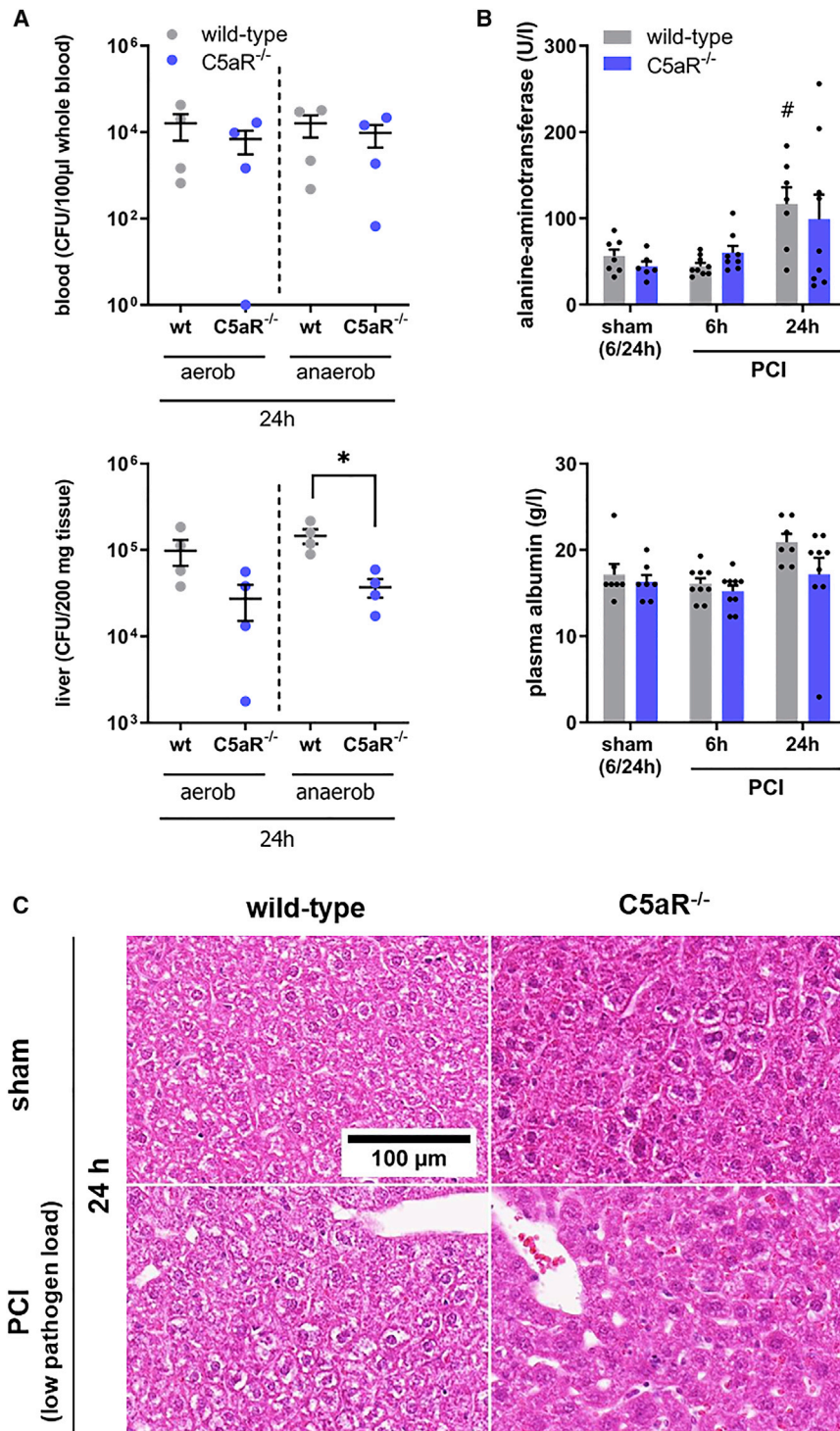


Figure 2. C5a1 Deficiency (C5aR^{-/-}) Improves Bacterial Clearance and Attenuates Liver Damage in a Mild Sepsis Model

(A) For bacteremia no differences were observed, whereas lower bacterial translocation into liver tissue was found in C5aR^{-/-} mice compared to wild-type mice subjected to a low pathogen load. Individual data (points), mean (line) and error (SEM) is presented. **Significance ($p < 0.05$), Student's *t* test. (B) Established clinical parameter (alanine aminotransferase) to monitor liver dysfunction or organ damage during septic insult indicated minor differences over time between wild-type and C5aR^{-/-} mice. Mean barplot + SEM and individual data points presented. #Significant ($p < 0.05$) to wild-type sham control, one-way ANOVA (Tukey test correction). (C) Histological staining of liver tissue showed no hepatocellular necrosis in wild-type and C5aR^{-/-} mice subjected to a low pathogen load.

icantly increased in wild-type mice compared to C5aR^{-/-} (Figure S3). The liver function was impaired in wild-type mice despite that no histologically evident damage occurred (Figure 2C).^{19,27}

Bilirubin was not significantly altered, confirming previous observations that identify total bilirubin as a marker with rather low sensitivity (Figure 3A). Mass spectroscopic analysis of conjugated and unconjugated bile acids in liver tissue and plasma from wild-type and knockout mice depicted an early drop of conjugated bile acids followed by an accumulation of conjugated and unconjugated bile acids, which was absent in C5aR^{-/-} mice (Figures 3B and S4).

At 24 h after peritoneal infection, a significantly decreased metabolic activity (i.e., bile acid conjugation) in wild-type but not C5aR^{-/-} animals was observed (Figure 3C).

The metabolic and excretory capacity of the hepatocytes was investigated additionally by intravital microscopy. Hepatic NAD(P)H autofluorescence and the hepatic elimination of DY-635²⁷ had been quantified by intravital microscopy to further investigate hepatocellular damage and dysfunction. Both the intensities of NAD(P)H and DY-635 were objectively

quantified by an automated image analysis procedure based on the segmentation of hepatocytes and evaluating the kinetics of DY-635 uptake and elimination over time by the classification of the curve shapes (Figure 3D).

local neutrophils in the liver, but 6 h after infection the cell number already increased to the level of wild-type mice with sepsis. At a late time point in this model (96 h), which is dominated by organ damage, the infiltration of polymorph nuclear positive (PMN⁺) cells was signif-

icantly increased in wild-type mice compared to C5aR^{-/-} (Figure S3). The liver function was impaired in wild-type mice despite that no histologically evident damage occurred (Figure 2C).^{19,27}

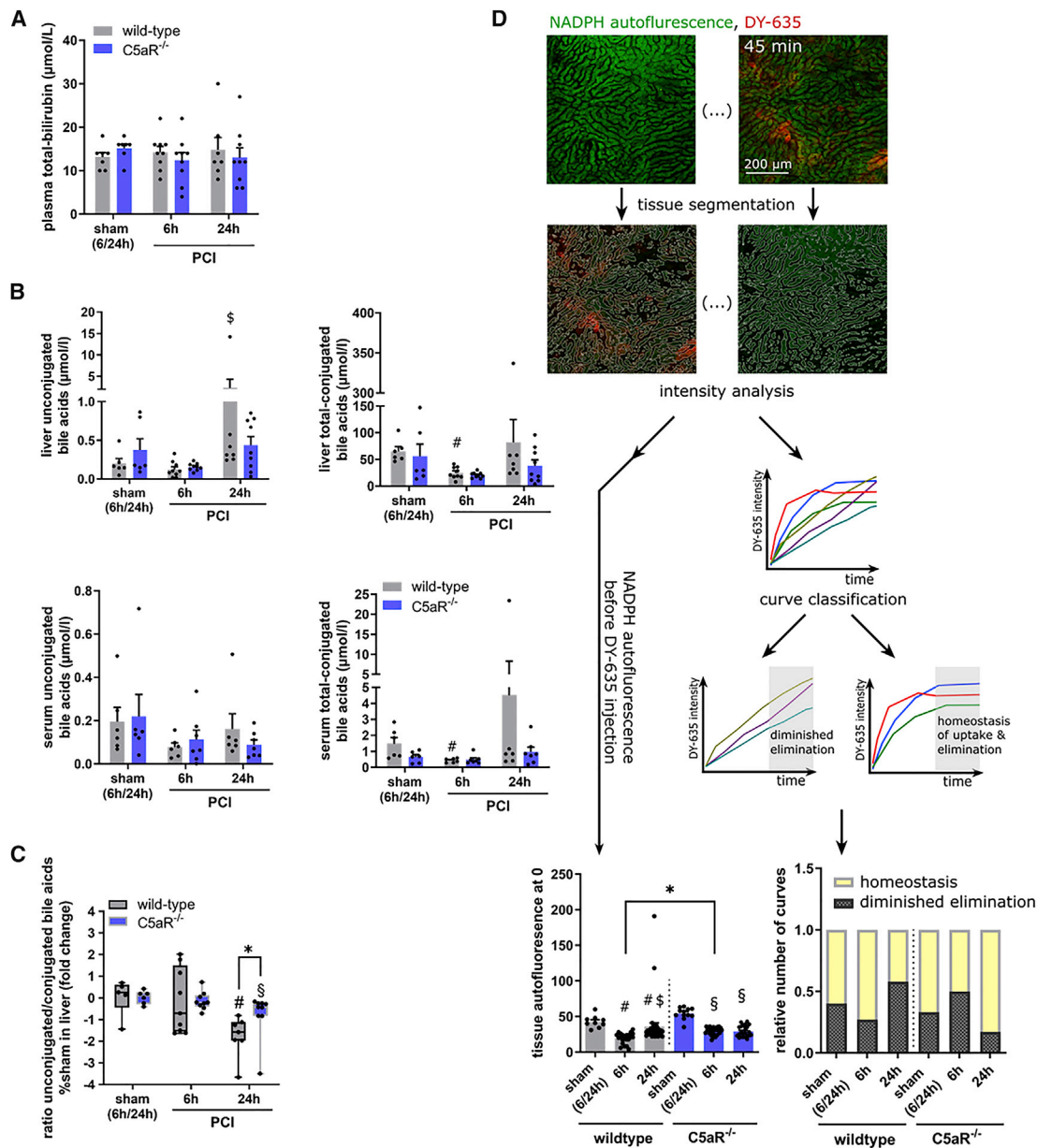


Figure 3. C5aR^{-/-} Attenuates Excretory Liver Dysfunction in a Mild Sepsis Model in Mice

(A) Whereas total bilirubin showed no differences, (B) a higher increase of unconjugated and total conjugated bile acids was monitored in wild-type mice compared to C5aR^{-/-} mice subjected to low pathogen load in serum and liver. Data depicted as mean bar plot + SEM and individual data points. (C) The ratio of unconjugated to conjugated bile acids (Tukey’s boxplot with individual data points) displayed a significant decrease in wild-type mice. Excretory liver dysfunction was more pronounced in wild-type mice compared to C5aR^{-/-} mice. (D) Schematic illustration of basic image processing workflow to obtain NADPH autofluorescence intensities and DY-635 elimination curves. The curve shape had been classified according to their biomedical interpretation and plotted according to their relative occurrence over all analyzed animals. A constant linear increase reflects a continuous DY-635 accumulation in hepatocytes and diminished elimination. An efficient DY-635 elimination is depicted by a homeostasis of DY-635 uptake and elimination in hepatocytes within 45 min. [#]Significant to wild-type sham control, [§]significant to wild-type 6 h, [§]significant to C5aR^{-/-} sham control with $p < 0.05$, (A) one-way ANOVA (Tukey test correction), or (B–D) Kruskal-Wallis test (Dunn’s test correction). *Statistical significance ($p < 0.05$) between wild-type and C5aR^{-/-} applying (C) Student’s t test or (D) Wilcoxon-Mann-Whitney.

The elimination of DY-635 was observed over 45 min by confocal intravital microscopy. After intravenous injection, DY-635 is rapidly accumulating in the liver. While DY-635 plasma levels

are decreasing, the hepatocellular concentration is increasing. If the hepatocytes efficiently eliminate DY-635, equilibrium of uptake (into hepatocytes) and elimination (from hepatocytes into

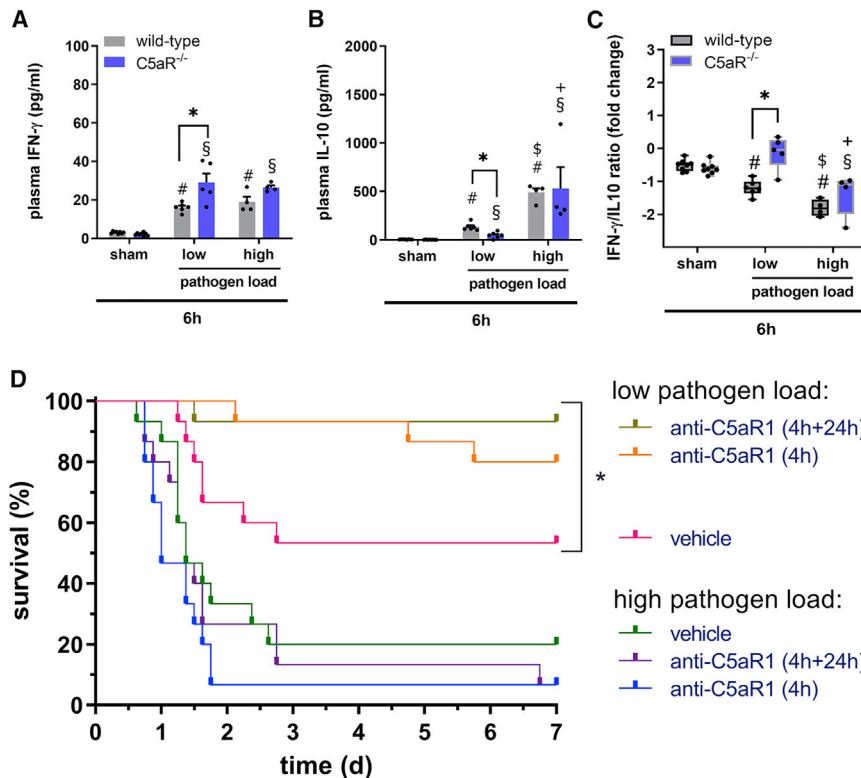


Figure 4. C5ar1 Deficiency Promotes the Shift from Innate to Adaptive Immune Response

(A and B) Significantly higher plasma IFN- γ (A) and significantly lower plasma IL-10 (B) levels were found in C5aR^{-/-} mice compared to wild-type mice subjected to low pathogen load, whereas C5aR^{-/-} mice and wild-type mice showed minor differences when subjected to high pathogen load. (C) IFN- γ /IL-10 ratio, described as biomarker for the assessment of immune dysfunction, continued to decrease from mild to severe infection in wild-type mice. In C5aR^{-/-} mice subjected to low pathogen load, a significantly higher ratio was found, whereas the ratio did not differ between the groups when subjected to high pathogen load. (D) Survival rate and anti-C5aR1 treatment (anti-C5aR1 injection 4 h after PCI, anti-C5aR1 injection 4 h and 24 h after PCI, vehicle control) in mice subjected to low (mild to moderate sepsis) and high pathogen load (severe sepsis). Blocking C5aR1 is associated with a beneficial outcome in mild to moderate sepsis. (A-C) Data are depicted as Tukey boxplot with overlaid individual data points. #Significant to wild-type sham control, \$significant to wild-type 6 h, §significant to C5aR^{-/-} sham control, +significant to C5aR^{-/-} 6 h with $p < 0.05$ (A and B) Kruskal-Wallis test (Dunn's test correction), or (C) one-way ANOVA (Tukey test correction). *Statistical significance ($p < 0.05$) between wild-type and C5aR^{-/-} by means of (A and B) Wilcoxon-Mann-Whitney test or (C) Student's t test; (D) log-rank test, $p < 0.05$, 15 mice/group.

the bile) is reached. The occurrence of this homeostasis is characteristic of a physiologic biotransformation in the liver. In case of excretory liver failure, the hepatocytes will accumulate DY-635. Being unable to eliminate the dye into the bile, the intracellular concentration in this experiment is constantly rising over the observation period (45 min), resulting in a constant linear increase. Curves that reach a saturation (representing the equilibrium of DY-635 uptake and elimination) and those that constantly increase (diminished elimination) are then automatically detected and classified from the intensity analysis. Their frequency of occurrence was plotted afterward and reflects changes in the overall elimination capacity of the liver.

Our analysis indicates a protection of the excretory liver function at 24 h in C5aR^{-/-} mice in comparison to wild-type animals (Figure 3D). These observations are in line with and further supported by the results obtained in the quantification of bile acids (i.e., the accumulation of unconjugated bile acid in wild-type but not C5aR^{-/-} mice after 24 h).

The NAD(P)H autofluorescence may be interpreted as surrogate for the hepatocellular redox potential and thus metabolic activity or vitality.²⁷ A drop in NAD(P)H autofluorescence was observed in both BALB/c wild-type and C5aR^{-/-} mice. NAD(P)H levels in the liver of wild-type mice were further significantly lower after 6 h sepsis compared to C5aR^{-/-}, which supports the notion of reduced meta-

bolic activity leading to the subsequent drop in bile acid conjugation observed in wild-type mice after 24 h (Figure 3C).

Together, these findings suggest the protection of C5aR^{-/-} mice from excretory liver failure during the course of infection, which is most likely due to different immune responses that the animals have to cope with during infection.

C5aR1 Function Correlates with the Pro-inflammatory to Anti-inflammatory Switch in Sepsis

The pro-inflammatory response did not differ between wild-type and C5aR knockout mice, as shown by the levels of circulating cytokines (IL-6, tumor necrosis factor alpha [TNF- α], and MCP-1) or C5a (Figure S5). However, a significant decrease of IL-10 and an increase of interferon- γ [IFN- γ] might indicate an early switch to the adaptive immune response in C5aR knockouts. Notably, this switch in the immune response did not occur in animals subjected to high pathogen loads (Figures 4A and 4B). The ratio of IFN- γ to IL-10 was previously described as a measure for the general inflammatory response during systemic infections and the ability of the immune cell to control pathogen invasion.^{28,29} Figure 4C depicts this ratio for the models with low and high load, indicating protection of C5aR^{-/-} mice from a deregulated host response caused by a mild infection. During severe infection, however, this protection disappears in accordance with a lack of survival benefit (Figures 1B and 1C). To corroborate these results, animals have been subjected to a low or high pathogen burden

with an anti-C5ar1-blocking antibody (Figure 1D). Similar to the experiments in knockout mice, treatment with the antibody protected animals subjected to a low pathogen burden but did not affect severely sick animals (Figure 4D). Together, the survival benefits of the C5aR^{-/-} mice and the anti-C5ar1-treated BALB/c mice in the low-dose PCI model correlate with a fortified immune response of the C5ar1-deficient animals, suggesting an immunosuppressive function of C5a signaling in these settings.

DISCUSSION

Efficient treatment of the deregulated host response is a long-term goal in sepsis research. Many clinical trials targeting the initial overwhelming immune response (e.g., by sequestering cytokines) finally failed.³⁰ Previous studies in animal models of sepsis suggest the complement system as a promising target for the development of novel therapeutic approaches.³¹

The knockout or blocking of C5a receptors before inducing experimental sepsis through cecal ligation and puncture or intraperitoneal *Neisseria meningitidis* and iron-dextran co-administration reduced mortality in mice.^{15,32} Also blocking the anaphylatoxin C5a protected from the development of multiorgan failure in rats.⁹ In contrast, a 12-h delayed anti-C5ar1 treatment did not exert beneficial effects.¹⁵ Our data depict that C5aR^{-/-} mice are protected from sepsis in a low-pathogen-dose sepsis model. When mice were infected with high pathogen loads, the C5aR^{-/-} (or the anti-C5ar1 block) did not exert protective effects. C5ar1 block in wild-type mice after 4 h, as well as 4 and 24 h, after inducing sepsis by peritoneal contamination and infection confirmed the positive influence on the outcome in C5aR^{-/-} mice administered to low pathogen loads only. These findings highlight the importance of the early timing of a C5ar1 blocking strategy and motivate an individualized approach according to the severity of the infection.

In a prospective observational study circulating IL-10, soluble CD25, and IFN- γ were found to add prognostic value for an early diagnosis of bacteremia.³³ Recently, particularly the IFN- γ /IL-10-ratio was described as a marker indicating the host's control over the immune response and infection.^{28,29} The increased IFN- γ /IL-10 ratio and cytokine profiles in C5ar1-deficient mice, challenged by the low-dose sepsis model, supports the idea that C5a signaling under the given conditions is fulfilling an immunosuppressive function. Under these immunosuppressive conditions, pathogen-induced organ damage might cause increased mortality of wild-type animals. In contrast, the increased survival of C5aR^{-/-} animals might be explained by more efficient resistance responses of the innate and adaptive immune system emerging at high IFN- γ /IL-10 ratios. This hypothesis is strongly supported by the lower bacterial load in C5ar1-deficient animals, at least in the liver.

The effective control of infection in C5aR^{-/-} mice might be primarily attributed to decreased receptor signaling in immune cells and also parenchymal cells. The presence of the C5ar1 on parenchymal cells was reported before by several authors,^{18,20,34,35} and we showed its in-

duction also in hepatocytes during infection. The given studies suggest that both C5ar1-dependent and -independent complement signaling activities are important mediators of inflammation in immune and parenchymal cells during sepsis. C5ar1 independent effects might be mediated through activation of the C5ar2 receptor. The C5ar2 receptor was described as a decoy receptor and negative regulator of C5ar1 leading to immunosuppression. However, the mechanisms of how the activation of C5ar2 leads to a negative regulation of C5a-induced immune functions are not yet elucidated.^{14,16} In addition, the physiologic effects of its activation are currently controversially discussed and vary between different animal models of inflammation.^{15,17}

The dysregulation of the immune response during systemic infection leads to organ impairment and failure. Liver function in sepsis is affected indirectly by resident and invading macrophages and neutrophils during an infection-causing tissue necrosis.^{22,24} Early liver failure in sepsis, especially in models with low severity, is rarely accompanied by tissue necrosis but rather by direct effects on pathophysiologic signaling mechanisms in hepatocytes. Our study depicts that the C5ar1 is upregulated on immune cells but also on parenchymal hepatocytes in the liver. Lower bacterial translocation into liver tissue accompanied by decreased immune cell recruitment reduces the harmful effects on the liver of C5a in the C5aR^{-/-}. The C5aR^{-/-} also maintains bile acid conjugation in a low-dose sepsis model during the acute phase. However, the activation of the adaptive immune response, exemplified by an increased IFN γ /IL-10 ratio, reduced protective effects of the C5aR^{-/-} in the later phase (24 h) and is accompanied by decreased excretory liver function.

The activation of C5a receptors by C5a exhibits ambivalent effects on the immune response during the acute phase of inflammation.⁴ The loss of these overall protective effects with reduced tissue damage and retained organ function during infection in the high-dose model of the C5aR^{-/-} mice underline the concept of pathogen dose-related effects and other stressors in infectious diseases, where the interaction of hyperinflammation and immunosuppression play a crucial role.³⁶ Thus, under conditions where the infection does not immediately overwhelm the host and an adequate adaptive immune response is achieved, the C5aR^{-/-} leads to an overall beneficial effect.

Our results uncover an immunosuppressive function of C5ar1 in sepsis. The data propose the IFN- γ /IL-10 ratio as a promising biomarker to identify the immune status of sepsis patients. In addition, C5ar1 blocking therapy was introduced as a novel therapeutic concept in sepsis.

MATERIALS AND METHODS

Animals

Handling of mice and experimental procedures were conducted in accordance with the animal welfare legislation of the state of Thuringia. BALB/c and C.129S4(B6)-C5ar1^{tm1Cge/J} (C5aR^{-/-}) were bred and housed at the animal facility of the Jena University Hospital. The genotypes were confirmed by genotyping.

Peritoneal Contamination and Infection

BALB/c and C5aR^{-/-} mice were infected by injecting a standardized human stool suspension, adapting severity by using several doses per g BW. In some groups, animals received adjunctive treatment with meropenem or an anti-C5aR [clone 20/70] antibody. For the low-dose sepsis model, 0.8 µL per g BW was used. For the high-dose sepsis model, 1.25 µL per g BW without antibiotic treatment and 3.5 µL per g BW with antibiotic treatment (meropenem: 25 mg per kg BW in 10 µL per g BW) were applied, starting 6 h after infection, every 12 h for 3 days after sepsis induction. 0.6 mg kg⁻¹ anti-C5aR1 ([clone 20/70] (immunoglobulin G2b [IgG2b] to mouse C5aR1 (LifeSpan Bioscience, USA) or vehicle (PBS) was administered intravenously 4 h or 4 and 24 h after infection. The anti-C5aR1 [20/70] antibody used is well established for *in vivo* C5aR1-blocking experiments (e.g., Rittirsch et al.¹⁵). Different representative lots have been tested and shown to neutralize complement receptor C5aR activation (e.g., Godau et al.³⁷ and Mehta et al.³⁸). Animals were scored every 3 h, applying the clinical severity score described before.²⁶ Plasma and tissue were harvested in animals 6 and 24 h after the infection was established. Anesthetized mice (Isoflurane, 2.5 vol%) were laparotomized, blood was taken by heart puncture, and further tissue was harvested.

Intravital Microscopy and Image Analysis

Intravital microscopy was performed on BALB/c and C5aR^{-/-} mice 6 and 24 h after infection, as described previously, using DY-635 as a marker to analyze liver function.^{23,27,39} Microscopy image analysis was done by a customized Python pipeline with the help of the scikit-image library.⁴⁰ Intensities of DY-635 and NAD(P)H autofluorescence were analyzed at different time points. In order to exclude contributions from the background, the tissue (hepatocytes) area was segmented based on the NAD(P)H autofluorescence channel by (1) smoothing each image with a Gaussian filter (with width $\sigma = 1 \mu\text{m}$), (2) thresholding the intensities by Otsu's method, and (3) performing morphological opening and closing. The DY-635 and NAD(P)H intensities in each image were characterized by the median intensities computed over the tissue area. The integrated DY-635 intensity was computed for each time series as the average of DY-635 intensities of all time points from 0 to 60 min. The autofluorescence ratio was computed as the ratio between the average NAD(P)H intensity in the interval from 45 to 60 min and NAD(P)H intensity at time point 0 min. To analyze the DY-635 uptake dynamics and the DY-635 curve shape, the median DY-635 intensities were grouped into time intervals of 15 min (0 min, 0.5–15 min, 15.5–30 min, 30.5–45 min, 45.5–60 min), and the average intensity was computed for each time interval. The curves were classified into three groups according to their shape. The curves with maximum DY-635 intensity less than or equal to 10 gray levels (out of 255, 8 bit) were classified as “no uptake.” The curves were considered to be “saturated” if the maximum intensity was achieved during the first 15 min or the intensity at 15 min was higher than 80% of the maximum intensity. All remaining curves were classified as “linear increase.”

Histological Staining

Representative liver tissue was formalin fixed from sham and septic BALB/c and C5aR^{-/-} mice for 12–24 h in neutral-buffered formalde-

hyde and paraffin embedded (FFPE). Dehydration and paraffin embedding were automatically processed (Hypercenter; Shandon, Frankfurt, Germany). 4-µm-thick sections from formalin-fixed and paraffin-embedded organ tissues were cut, mounted, and deparaffinized. Hematoxylin and eosin-stained liver sections were imaged on a NanoZoomer (Hamamatsu). Neutrophils were stained 1 h at room temperature using rabbit polyclonal PMN (Gentaur GmbH, Germany) diluted 1:200 in 10% BSA in Tris-buffered saline (TBS). Then, the tissue was washed and incubated for another hour with AlexaFluor568 conjugated donkey anti-rabbit IgG (H+L) (Thermo Fisher Scientific) diluted in 10% BSA in TBS. Slides were washed again and counterstained with H333342 (Sigma Aldrich) for 5 min before mounting using RotiMount (Carl Roth). C5aR1 was stained in spleen and liver tissue of sham and septic BALB/c and C5aR^{-/-} mice. From the paraffin blocks, 4 µm sections were prepared and floated onto positively charged slides. C5aR1 immunostaining was performed by an indirect peroxidase labeling method as previously described.⁴¹ Briefly, sections were dewaxed, microwaved in 10 mM citric acid (pH 6.0) for 16 min at 600 W, and then incubated with the primary antibody (rabbit anti-mouse C5aR1 antibody 5474, Thermo Fisher Scientific, Waltham, MA, USA; concentration: 0.5 µg/mL) at 4°C overnight.

Cytokine Quantification

Cytokines were quantified from EDTA plasma. Samples were analyzed from sham and septic animals ($n \geq 3/\text{group}/\text{time point}$) for quantification of IL-6, IL-10, TNF- α , MCP-1, and IFN- γ using the flow cytometric bead assay kit (CBA) according to the manufacturer's instructions (mouse inflammation kit; BD Biosciences, Heidelberg, Germany). Samples were measured using the flow cytometer BD FACSCalibur (BD Biosciences, San Jose, CA, USA). Data were calculated with FCAP Array v1.0.1 from BD Biosciences for CBA.

Biochemical Analysis

For plasma, the collected supernatant was centrifuged at $2,000 \times g$ for 10 min at 4°C and stored at -80°C for later analyses. The activity of liver enzymes ALT, aspartate aminotransferase (AST), lactate dehydrogenase (LDH), lactate, albumin, and total bilirubin were analyzed using the automated clinical chemistry analyzer (Fuji Dri-Chem 3500i, Sysmex, Norderstedt, Germany).

Bacterial Burden

Blood and liver tissue were collected from BALB/c and C5aR knockout mice 24 h following PCI ($n = 4/\text{group}$) for analysis of the bacterial burden. 20 µL of whole blood, and dilutions, were inoculated on CBA and Schaedler agar. CBA plates were incubated at 37°C for 24 h under aerobic conditions. Schaedler agar plates were incubated at 37°C for 48 h under anaerobic conditions. Total CFU counts were evaluated with consideration of blood volume or normalized to wet weight of organs.

Bile Acid Analysis

20 bile acids were determined in serum and from liver tissue lysates according to the manufacturer's protocol (Bile Acids kit, Biocrates

Life Science AG, Innsbruck, Austria) on an Agilent 1200 high-performance liquid chromatography system (Agilent Technologies GmbH, Santa Clara, CA, USA) with a CTC-PAL autosampler (CTC Analytics AG, Zwingen, Switzerland) coupled to an API 4000 Triple Quadrupole mass spectrometer with electrospray ionization source (AB Sciex, Framingham, MA, USA) and the Analyst 1.6.2 software (AB Sciex, Framingham, MA, USA). In brief, 10 μ L internal standards were pipetted onto the spots of the kit plate and were dried 5 min at room temperature in a nitrogen evaporator drying unit. After adding 10 μ L calibration standard, quality control, serum or liver tissue lysate (supernatant of in a ball mill homogenized tissue [30 mg] with a 90 μ L mixture of ethanol/0.01 M phosphate puffer [85/15 v/v]; Merck, Darmstadt, Germany) the plate was dried again 20 min under nitrogen. 100 μ L methanol (high performance liquid chromatography [HPLC] grade, Carl Roth, Karlsruhe, Germany) was pipetted to each spot and incubated for 20 min at 600 rpm at room temperature. The plate was centrifuged at $500 \times g$ for 2 min. The upper filter plate was removed, 60 μ L water (HPLC grade) was added to each well of the lower capture plate, and the plate was incubated on a shaker for 5 min at 450 rpm. Sample (10 μ L) was injected onto the ultra-high performance liquid chromatography (UHPLC) column included into the kit coupled to a C18/XB-C18 precolumn and eluted with solvent A (475 mL water [HPLC grade] + 25 mL 200 mM NH_4Ac stock solution [in water, Merck, Darmstadt, Germany]) + 75 μ L formic acid (Merck, Darmstadt, Germany) and solvent B (325 mL acetonitrile [LC-MS grade, Roth, Karlsruhe, Germany] + 150 mL methanol [HPLC grade, Roth, Karlsruhe, Germany] + 25 mL 200 mM NH_4Ac stock solution [in water, Merck, Darmstadt, Germany] + 75 μ L formic acid [Merck, Darmstadt, Germany]). Peaks were integrated and concentrations were obtained with Analyst 1.6.2. Evaluation of calibration curves, blanks, quality controls, and samples were accomplished in the MetIDQ software, an integral part of the kit.

Statistics

Statistical analyses were done with GraphPad Prism Software v8.3.1 (San Diego, CA, USA). Descriptive statistical analyzes were performed for all obtained data. Survival data were displayed in Kaplan-Meier curves and analyzed by log rank test. Depending on assumed normality (Kolmogorov-Smirnov test) and number of groups, parametric tests or non-parametric tests were applied. The significance level was defined as $\alpha = 0.05$. Detailed information on the tests is given within the individual figure legends. Results are depicted as bar plots (mean + SEM) or boxplots (interquartile range [IQR], 0.25, 0.75; whiskers: min, max). Individual data points (n) are plotted over the bars/boxes, or the n was specified otherwise in the figure legend.

SUPPLEMENTAL INFORMATION

Supplemental Information can be found online at <https://doi.org/10.1016/j.ymthe.2020.09.008>.

AUTHOR CONTRIBUTIONS

All authors have seen and approved the final version of this manuscript and contributed to it as stated here: O.S. and A.T.P. performed

in vivo experiments. A.M. and M.T.F. analyzed image data. O.S., S.N., M.G., and S.U. analyzed tissue samples. R.K. guided statistical analysis. A.L. and S.S. performed histological analysis of C5ar1 expression. R.W., M.B., and A.T.P. supervised and guided the study. All authors wrote the manuscript.

CONFLICT OF INTEREST

All authors declare no competing interests.

ACKNOWLEDGMENTS

We acknowledge Petra Martinac and Ulrike Vetterling for supporting histological staining and animal experiments. We further thank Shivalie Duduskar for illustrating the graphical abstract and Johanna Isabelle Herold for her technical support with the bile acid quantification. This work was funded by the Federal Ministry for Education and Research, Center for Sepsis Control and Care (FKZ 01EO1002) and supported by the DFG-funded Collaborative Research Centre Poly-Target (SFB 1278, Project ID: 316213987) projects C03 and Z01.

REFERENCES

- Markiewski, M.M., DeAngelis, R.A., and Lambris, J.D. (2008). Complexity of complement activation in sepsis. *J. Cell. Mol. Med.* 12 (6A), 2245–2254.
- Rittirsch, D., Flierl, M.A., and Ward, P.A. (2008). Harmful molecular mechanisms in sepsis. *Nat. Rev. Immunol.* 8, 776–787.
- Schraufstatter, I.U., Khaldoyanidi, S.K., and DiScipio, R.G. (2015). Complement activation in the context of stem cells and tissue repair. *World J. Stem Cells* 7, 1090–1108.
- An, L.-L., Gorman, J.V., Stephens, G., Swerdlow, B., Warriner, P., Bonnell, J., Mustelin, T., Fung, M., and Kolbeck, R. (2016). Complement C5a induces PD-L1 expression and acts in synergy with LPS through Erk1/2 and JNK signaling pathways. *Sci. Rep.* 6, 33346.
- Yan, C., and Gao, H. (2012). New insights for C5a and C5a receptors in sepsis. *Front. Immunol.* 3, 368.
- Riedemann, N.C., Guo, R.-F., Gao, H., Sun, L., Hoesel, M., Hollmann, T.J., Wetsel, R.A., Zetoune, F.S., and Ward, P.A. (2004). Regulatory role of C5a on macrophage migration inhibitory factor release from neutrophils. *J. Immunol.* 173, 1355–1359.
- Wrann, C.D., Tabriz, N.A., Barkhausen, T., Klos, A., van Griensven, M., Pape, H.C., Kendoff, D.O., Guo, R., Ward, P.A., Krettek, C., and Riedemann, N.C. (2007). The phosphatidylinositol 3-kinase signaling pathway exerts protective effects during sepsis by controlling C5a-mediated activation of innate immune functions. *J. Immunol.* 178, 5940–5948.
- Czermak, B.J., Sarma, V., Pierson, C.L., Warner, R.L., Huber-Lang, M., Bless, N.M., Schmal, H., Friedl, H.P., and Ward, P.A. (1999). Protective effects of C5a blockade in sepsis. *Nat. Med.* 5, 788–792.
- Huber-Lang, M., Sarma, V.J., Lu, K.T., McGuire, S.R., Padgaonkar, V.A., Guo, R.F., Younkin, E.M., Kunkel, R.G., Ding, J., Erickson, R., et al. (2001). Role of C5a in multi-organ failure during sepsis. *J. Immunol.* 166, 1193–1199.
- Guo, R.-F., Riedemann, N.C., Bernacki, K.D., Sarma, V.J., Laudes, I.J., Reuben, J.S., Younkin, E.M., Neff, T.A., Paulauskis, J.D., Zetoune, F.S., and Ward, P.A. (2003). Neutrophil C5a receptor and the outcome in a rat model of sepsis. *FASEB J.* 17, 1889–1891.
- Bosmann, M., Sarma, J.V., Atefi, G., Zetoune, F.S., and Ward, P.A. (2012). Evidence for anti-inflammatory effects of C5a on the innate IL-17A/IL-23 axis. *FASEB J.* 26, 1640–1651.
- Seow, V., Lim, J., Iyer, A., Suen, J.Y., Ariffin, J.K., Hohenhaus, D.M., Sweet, M.J., and Fairlie, D.P. (2013). Inflammatory responses induced by lipopolysaccharide are amplified in primary human monocytes but suppressed in macrophages by complement protein C5a. *J. Immunol.* 191, 4308–4316.
- de Haas, C.J.C., Veldkamp, K.E., Peschel, A., Weerkamp, F., Van Wamel, W.J.B., Heezius, E.C.J.M., Poppelier, M.J., Van Kessel, K.P., and van Strijp, J.A. (2004).

- Chemotaxis inhibitory protein of *Staphylococcus aureus*, a bacterial antiinflammatory agent. *J. Exp. Med.* 199, 687–695.
14. Gao, H., Neff, T.A., Guo, R.-F., Speyer, C.L., Sarma, J.V., Tomlins, S., Man, Y., Riedemann, N.C., Hoesel, L.M., Younkin, E., et al. (2005). Evidence for a functional role of the second C5a receptor C5L2. *FASEB J.* 19, 1003–1005.
 15. Rittirsch, D., Flierl, M.A., Nadeau, B.A., Day, D.E., Huber-Lang, M., Mackay, C.R., Zetoune, F.S., Gerard, N.P., Cianflone, K., Köhl, J., et al. (2008). Functional roles for C5a receptors in sepsis. *Nat. Med.* 14, 551–557.
 16. Wang, R., Lu, B., Gerard, C., and Gerard, N.P. (2016). C5L2, the Second C5a Anaphylatoxin Receptor, Suppresses LPS-Induced Acute Lung Injury. *Am. J. Respir. Cell Mol. Biol.* 55, 657–666.
 17. Chen, N.-J., Mirtsos, C., Suh, D., Lu, Y.-C., Lin, W.-J., McKerlie, C., Lee, T., Baribault, H., Tian, H., and Yeh, W.C. (2007). C5L2 is critical for the biological activities of the anaphylatoxins C5a and C3a. *Nature* 446, 203–207.
 18. Riedemann, N.C., Guo, R.-F., Neff, T.A., Laudes, I.J., Keller, K.A., Sarma, V.J., Markiewski, M.M., Mastellos, D., Strey, C.W., Pierson, C.L., et al. (2002). Increased C5a receptor expression in sepsis. *J. Clin. Invest.* 110, 101–108.
 19. Kramer, L., Jordan, B., Druml, W., Bauer, P., and Metnitz, P.G.H.; Austrian Epidemiologic Study on Intensive Care, ASDI Study Group (2007). Incidence and prognosis of early hepatic dysfunction in critically ill patients—a prospective multicenter study. *Crit. Care Med.* 35, 1099–1104.
 20. Koleva, M., Schlaf, G., Landmann, R., Götz, O., Jungermann, K., and Schieferdecker, H.L. (2002). Induction of anaphylatoxin C5a receptors in rat hepatocytes by lipopolysaccharide in vivo: mediation by interleukin-6 from Kupffer cells. *Gastroenterology* 122, 697–708.
 21. Strey, C.W., Markiewski, M., Mastellos, D., Tudoran, R., Spruce, L.A., Greenbaum, L.E., and Lambris, J.D. (2003). The proinflammatory mediators C3a and C5a are essential for liver regeneration. *J. Exp. Med.* 198, 913–923.
 22. Laschke, M.W., Menger, M.D., Wang, Y., Lindell, G., Jeppsson, B., and Thorlacius, H. (2007). Sepsis-associated cholestasis is critically dependent on P-selectin-dependent leukocyte recruitment in mice. *Am. J. Physiol. Gastrointest. Liver Physiol.* 292, G1396–G1402.
 23. Recknagel, P., Claus, R.A., Neugebauer, U., Bauer, M., and Gonnert, F.A. (2012). In vivo imaging of hepatic excretory function in the rat by fluorescence microscopy. *J. Biophotonics* 5, 571–581.
 24. Recknagel, P., Gonnert, F.A., Westermann, M., Lambeck, S., Lupp, A., Rudiger, A., Dyson, A., Carré, J.E., Kortgen, A., Krafft, C., et al. (2012). Liver dysfunction and phosphatidylinositol-3-kinase signalling in early sepsis: experimental studies in rodent models of peritonitis. *PLoS Med.* 9, e1001338.
 25. Gressner, O.A., Koch, A., Sanson, E., Trautwein, C., and Tacke, F. (2008). High C5a levels are associated with increased mortality in sepsis patients—no enhancing effect by actin-free Gc-globulin. *Clin. Biochem.* 41, 974–980.
 26. Gonnert, F.A., Recknagel, P., Seidel, M., Jbeily, N., Dahlke, K., Bockmeyer, C.L., Winning, J., Lösche, W., Claus, R.A., and Bauer, M. (2011). Characteristics of clinical sepsis reflected in a reliable and reproducible rodent sepsis model. *J. Surg. Res.* 170, e123–e134.
 27. Schaarschmidt, B., Vlačić, S., Medyukhina, A., Neugebauer, S., Nietzsche, S., Gonnert, F.A., Rödel, J., Singer, M., Kiehntopf, M., Figge, M.T., et al. (2018). Molecular signatures of liver dysfunction are distinct in fungal and bacterial infections in mice. *Theranostics* 8, 3766–3780.
 28. Olu Akinshipe, B., Ehiaghe, A.F., Nwaobi, A.C., Adedeji, A.B., and Okpali, H.O. (2017). The Patterns of Interferon-Gamma and Interleukin-10 Production as a Potential Immunological Biomarker for the Outcome of Mycobacterium Tuberculosis Infection. *International Journal of Immunology* 5, 97–105.
 29. Koenig, R., Kolte, A., Ahlers, O., Oswald, M., Roell, D., Dimopoulos, G., Tsangaris, I., Antoniadou, E., Bogatsch, H., Löffler, M., et al. (2018). Use of IFN γ /IL10 ratio for stratification of hydrocortisone therapy in patients with septic shock: Supplementary material. *bioRxiv*. <https://doi.org/10.1101/502864>.
 30. Riedemann, N.C., Guo, R.-F., and Ward, P.A. (2003). The enigma of sepsis. *J. Clin. Invest.* 112, 460–467.
 31. Ward, P.A. (2012). New approaches to the study of sepsis. *EMBO Mol. Med.* 4, 1234–1243.
 32. Herrmann, J.B., Muenstermann, M., Strobel, L., Schubert-Unkmeir, A., Woodruff, T.M., Gray-Owen, S.D., Klos, A., and Johswich, K.O. (2018). Complement C5a Receptor 1 Exacerbates the Pathophysiology of *N. meningitidis* Sepsis and Is a Potential Target for Disease Treatment. *MBio* 9, e01755-17.
 33. Matera, G., Puccio, R., Giancotti, A., Quirino, A., Pulicari, M.C., Zicca, E., Caroleo, S., Renzulli, A., Libertò, M.C., and Focà, A. (2013). Impact of interleukin-10, soluble CD25 and interferon- γ on the prognosis and early diagnosis of bacteremic systemic inflammatory response syndrome: a prospective observational study. *Crit. Care* 17, R64.
 34. Haviland, D.L., McCoy, R.L., Whitehead, W.T., Akama, H., Molmenti, E.P., Brown, A., Haviland, J.C., Parks, W.C., Perlmutter, D.H., and Wetsel, R.A. (1995). Cellular expression of the C5a anaphylatoxin receptor (C5aR): demonstration of C5aR on nonmyeloid cells of the liver and lung. *J. Immunol.* 154, 1861–1869.
 35. Schieferdecker, H.L., Schlaf, G., Koleva, M., Götz, O., and Jungermann, K. (2000). Induction of functional anaphylatoxin C5a receptors on hepatocytes by in vivo treatment of rats with IL-6. *J. Immunol.* 164, 5453–5458.
 36. Bauer, M., Weis, S., Netea, M.G., and Wetzker, R. (2018). Remembering Pathogen Dose: Long-Term Adaptation in Innate Immunity. *Trends Immunol.* 39, 438–445.
 37. Godau, J., Heller, T., Hawlisch, H., Trappe, M., Howells, E., Best, J., Zwirner, J., Verbeek, J.S., Hogarth, P.M., Gerard, C., et al. (2004). C5a initiates the inflammatory cascade in immune complex peritonitis. *J. Immunol.* 173, 3437–3445.
 38. Mehta, G., Scheinman, R.I., Holers, V.M., and Banda, N.K. (2015). A New Approach for the Treatment of Arthritis in Mice with a Novel Conjugate of an Anti-C5aR1 Antibody and C5 Small Interfering RNA. *J. Immunol.* 194, 5446–5454.
 39. Press, A.T., Butans, M.J., Haider, T.P., Weber, C., Neugebauer, S., Kiehntopf, M., Schubert, U.S., Clemens, M.G., Bauer, M., and Kortgen, A. (2017). Fast simultaneous assessment of renal and liver function using polymethine dyes in animal models of chronic and acute organ injury. *Sci. Rep.* 7, 15397.
 40. van der Walt, S., Schönberger, J.L., Nunez-Iglesias, J., Boulogne, F., Warner, J.D., Yager, N., Goullart, E., and Yu, T.; scikit-image contributors (2014). scikit-image: image processing in Python. *PeerJ* 2, e453.
 41. Kaemmerer, D., Sängler, J., Arsenic, R., D'Haese, J.G., Neumann, J., Schmitt-Graeff, A., Wirtz, R.M., Schulz, S., and Lupp, A. (2017). Evaluation of somatostatin, CXCR4 chemokine and endothelin A receptor expression in a large set of paragangliomas. *Oncotarget* 8, 89958–89969.